J. Fluid Mech. (1970), *vol.* 40, *part* 1, *pp.* 127–148
Printed in Great Britain

The decay of perturbations in a radiating gas

By D. B. OLFE AND E. P. DEPLOMB
Department of the Aerospace and Mechanical Engineering Sciences,
University of California, San Diego

(Received 26 December 1968 and in revised form 19 March 1969)

The decay of perturbations in a radiating gas is analyzed by first carrying out complete solutions for the decay of initial sinusoidal perturbations in the temperature, gas velocity, and pressure. These sinusoidal perturbations are superposed to yield solutions for the decay of initial 'step' temperature profiles consisting of constant initial temperature perturbations inside finite planar, cylindrical and spherical regions, with zero initial temperature perturbations outside. In contrast to the sinusoidal case, which may be described by a single radiation parameter, the decay of the step profile is determined by both the optical depth of the initial profile and the Boltzmann number, which is inversely proportional to the blackbody radiative flux. As the limits of zero and infinite Boltzmann numbers are approached, constant-density and constant-pressure cooling expressions are recovered. For a broad range of intermediate and small Boltzmann numbers the cooling proceeds in time from a constant-density process to a constant-pressure process. This transition is produced by gasdynamic waves generated near the profile edges by the radiative cooling. The temperature near the profile centre may increase during the transition period.

1. Introduction

The decay of perturbations in a radiating gas has been the subject of a number of previous studies. Consideration of a sinusoidal perturbation proportional to $e^{i(\omega t - kx)}$ leads to a characteristic equation, which yields ω roots for a fixed wavenumber k, or k roots for a fixed frequency ω. Analyses of the ω roots (time-damped case) have been carried out for application to planetary and stellar atmospheres. The pure imaginary or 'thermal' ω root has been studied by Spiegel (1957), Goody (1964), Sasamori & London (1966) and Goody & Belton (1967). The additional two 'acoustic' ω roots have been investigated by Golitsyn (1963), Stein & Spiegel (1967) and Gille (1968).

Parallel analyses of the k roots of the characteristic equation (space-damped case) have been carried out by Prokof'ev (1957, 1961), Riazantsev (1959) and Vincenti & Baldwin (1962). Also, Smith (1957) and Calvert *et al.* (1966) have studied space-damping by extending Stokes's (1851) transparent gas analysis to crudely account for absorption effects. In addition to solving the characteristic equation for the k roots. Vincenti & Baldwin (1962) determine the relative amplitudes of the sinusoidal terms involving the k roots in order to form a complete solution for the problem of a semi-infinite radiating gas bounded by

a wall which undergoes sinusoidal oscillations in position and temperature. In § 2 of this paper we carry out the corresponding solution for the decay of sinusoidal perturbations in an infinite radiating gas by determining the relative amplitudes of the sinusoidal terms involving the three ω roots.

Baldwin (1962) has superposed space-damped sinusoidal waves to calculate the effect of radiative transfer on the propagation of an acoustic disturbance produced by impulsive wall motion. This problem has also been studied by Lick (1964) and Moore (1966). The disturbance produced by a step input of wall radiation was also discussed by Baldwin (1962), with further work carried out by Solan & Cohen (1966) and by Cogley (1968).

In § 3 of this paper we superpose time-damped sinusoidal waves to calculate the decay of initial 'step' temperature profiles consisting of constant temperature perturbations inside finite planar, cylindrical, and spherical regions, with zero initial temperature perturbations outside. In order to carry out specific calculations the initial pressure and gas velocity perturbations are taken to be zero, although other initial conditions could be included without complicating the calculations to any degree. The calculated temperature decay features and induced gas motions should be characteristic of other initial temperature, pressure and velocity profiles. On the other hand, the pure sinusoidal profile is a special, self-similar case which does not exhibit all of the decay features of the 'superposed profiles'.

The step profile decay considered in § 3 corresponds to the linearized steady flow problem of the temperature decrease in a free-mixing jet or wake. This correspondence requires that radiative transfer in the transverse direction dominates over radiative transfer in the flow direction, a condition which is usually valid. The equations for free-mixing flow with radiation have been described by Pai (1963), whereas Sforza & Porter (1968) have recently carried out calculations for the planar, constant-pressure case, including both radiation and heat conduction. Our calculations, which include the effects of pressure and gas velocity perturbations, thus represent a generalization of the calculations of Sforza & Porter, if heat conduction is neglected in their solution. The pure radiative cooling problem (without pressure or velocity perturbations) has also been studied by Vetlutski & Onufriev (1962) ,who consider both the linear and non-linear situations.

The non-linear, radiative cooling of the shocked gas produced by a strong explosion has been analyzed by Zel'dovich & Raizer (1967). Baltha & Viskanta (1968) have also recently investigated the non-linear cooling of a radiating gas surrounded by an absorbing cold gas. Since these non-linear analyses do not consider gasdynamic effects, our linearized calculation should provide qualitative information on induced pressure and velocity effects for such problems.

2. Sinusoidal perturbations

Linearization of the conservation equations for a radiating, perfect, inviscid gas yields the following expressions (see Vincenti & Kruger 1965):

$$A_S \equiv \frac{1}{a_0^2}\frac{\partial^2 \phi}{\partial t^2} - \frac{\partial^2 \phi}{\partial x_j \partial x_j} = \left(\frac{\gamma - 1}{\rho_0 a_0^2}\right)\frac{\partial q_j^{R'}}{\partial x_j}, \tag{1}$$

and
$$A_T \equiv \frac{\gamma}{a_0^2}\frac{\partial^2\phi}{\partial t^2} - \frac{\partial^2\phi}{\partial x_j \partial x_j} = -\frac{1}{T_0}\frac{\partial T'}{\partial t}, \tag{2}$$

where $a_0 = (\gamma R T_0)^{\frac{1}{2}}$ is the isentropic sound speed in the unperturbed gas, γ is the ratio of specific heats, T' is the temperature perturbation, and $\partial q_j^{R'}/\partial x_j$ represents the divergence of the net radiative flux. The gas velocity and pressure perturbations may be obtained from the potential function ϕ by means of the following derivatives
$$u_i' = \frac{\partial\phi}{\partial x_i}, \quad p' = -\rho_0\frac{\partial\phi}{\partial t}. \tag{3}$$

In this paper we deal explicitly with T', u_i', and p'. The density perturbation may be obtained from the equation of state for a perfect gas, i.e. ρ'/ρ_0 equals p'/p_0 minus T'/T_0. The quantities A_S and A_T are respectively the isentropic and isothermal wave operators applied to ϕ. Equations (1) and (2) were derived by Vincenti & Baldwin (1962), who studied the problem of the propagation of plane acoustic waves in a semi-infinite medium bounded by a wall undergoing sinusoidal perturbations in velocity and/or temperature. In order to point out similarities to the Vincenti & Baldwin analysis, the radiative decay problem will be first solved by using the differential approximation (Eddington approximation) for the radiative transfer in a gray gas.

The following differential equation for ϕ is obtained by combining (1) and (2) with the differential approximation for radiative transfer (see Vincenti & Kruger 1965)
$$\frac{\partial^3 A_S}{\partial t\,\partial x_j\,\partial x_j} + \left(\frac{16}{Bo}\right)\alpha_0 a_0 \frac{\partial^2 A_T}{\partial x_j\,\partial x_j} - 3\alpha_0^2\frac{\partial A_S}{\partial t} = 0, \tag{4}$$

where α_0 is the linear absorption coefficient evaluated at the unperturbed conditions T_0 and ρ_0. (As discussed in the previous studies, linearization of the equation of radiative transfer shows that the variation of the absorption coefficient may be neglected to lowest order.) In (4) Bo represents the Boltzmann number, a dimensionless convection-radiation parameter defined by
$$Bo \equiv \frac{\gamma R \rho_0 a_0}{(\gamma-1)\,\tilde{\sigma} T_0^3}, \tag{5}$$

where R is the gas constant and $\tilde{\sigma}$ is the Stefan–Boltzmann constant.

Substitution of a sinusoidal perturbation $\phi \propto e^{i(\omega t - kx)}$ into (4) gives a characteristic equation, which may be solved for either ω or k. The characteristic equation is cubic in terms of ω, and quadratic in terms of k^2. For the space-damped problem treated by Vincenti & Baldwin (1962), ω is fixed because the acoustic waves are generated at a wall which is oscillating in position and temperature at the fixed frequency ω. Expressed in terms of the dimensionless complex wave speeds $c \equiv -(ia_0/\omega)\,k$, the quadratic characteristic equation for c^2 yields the roots $\pm c_1$ and $\pm c_2$, with c_1 representing a 'modified classical' wave and c_2 representing a 'radiation induced' wave (see Vincenti & Baldwin 1962).

For the decay problem treated in this section, k is fixed. It is convenient to work with the non-dimensional frequency $\sigma \equiv (1/ika_0)\,\omega$ and a propagation vector $\mathbf{k}$ in the direction of the initial sinusoidal disturbance. Substitution of

$\phi \propto \exp(-\sigma k a_0 t + i\mathbf{k}.\mathbf{s})$ into (4) provides the following characteristic equation for σ:

$$\sigma^3 - \gamma\Gamma\sigma^2 + \sigma - \Gamma = 0, \tag{6}$$

where the non-dimensional radiation parameter is given by

$$\Gamma_{\text{approx.}} = \left(\frac{16}{Bo}\right)\left(\frac{Bu}{1+3Bu^2}\right), \tag{7}$$

with the subscript 'approx.' signifying that the differential approximation has been used. The Bouguer number $Bu \equiv \alpha_0/k = \alpha_0\lambda/2\pi$ is a dimensionless parameter which measures the opacity of the gas enclosed within a wavelength λ of the sinusoidal disturbance.

Characteristic equations equivalent to (6) have been analyzed by Golitsyn (1963), Stein & Spiegel (1967) and Gille (1968). As shown by these authors, the cubic equation (6) is appropriate even when the differential approximation and gray gas assumption are not made, i.e. linearization of the exact, non-gray radiative transfer equation and substitution of sinusoidal solutions yields (6). For a gray gas the exact expression for Γ is

$$\begin{aligned}\Gamma &= \left(\frac{16}{Bo}\right) Bu\left[1 - Bu\tan^{-1}\left(\frac{1}{Bu}\right)\right] \\ &= \left(\frac{16}{Bo}\right)\frac{1}{\kappa}\left[1 - \left(\frac{1}{\kappa}\right)\tan^{-1}\kappa\right],\end{aligned} \tag{8}$$

where $\kappa \equiv 1/Bu$ is a non-dimensional wave-number for the sinusoidal disturbance. The corresponding non-gray expressions for Γ may be obtained from Goody (1964) and Gille (1968).

Equation (8) shows that, for a gray gas, Γ is proportional to the blackbody emission (as measured by $16/Bo$) times an opacity function which measures the fraction of the blackbody radiation transferred between the temperature maxima and minima. This opacity function, shown in figure 1, has a maximum when $\kappa \equiv k/\alpha_0$ is of order unity because the maximum transfer of radiant energy will occur when the mean free path $(1/\alpha_0)$ is of the same order of magnitude as the distance $(1/k)$ between the temperature peaks in the sinusoidal disturbance. In the optically-thick limit ($\kappa \ll 1$) radiative transfer is small because emitted radiation is absorbed close to the point of emission, i.e. the radiation becomes trapped within a small fraction of the disturbance wavelength (thus the temperature maxima and minima do not directly exchange radiant energy). Radiative transfer becomes small in the optically thin limit because the radiation emitted from a disturbance wavelength becomes proportional to $1/\kappa Bo$, which is small when the gas is sufficiently transparent, i.e. when $\kappa \gg 1/Bo$.

The time-damping situation considered here is simpler than the space-damping case studied by Vincenti & Baldwin (1962), because the Boltzmann number Bo and the Bouguer number Bu are combined into a single radiation parameter Γ; in fact, even the non-gray problem involves only a single radiation parameter. This result was produced by the choice of a sinusoidal profile for the initial disturbance. For a sinusoidal profile the energy absorbed at a point,

as well as the energy emitted, is proportional to the local temperature perturbation at the point (see e.g. Smith 1957 or Golitsyn 1963). Therefore, the decaying disturbance retains its sinusoidal shape, and a change in Bu is equivalent to a corresponding change in Bo which produces the same net radiation loss (same Γ). On the other hand, the step profiles considered in § 3 (or any other non-sinusoidal profiles) do not decay through a sequence of self-similar profiles; in addition, both the Boltzmann number and the optical width of the initial step profile must be considered as separate parameters.

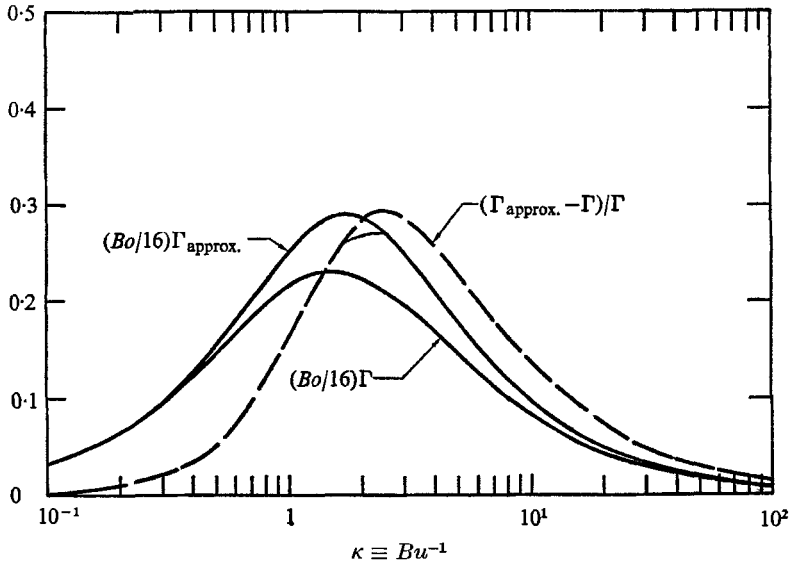

FIGURE 1. Exact and approximate radiation parameters for a gray gas as functions of the non-dimensional wave-number κ.

Let us now examine the roots to (6). The coefficients of the σ terms are such that there is one real root σ_0 and a pair of complex conjugate roots $\sigma_\pm = \sigma_r \pm i\sigma_i$, where σ_r and σ_i are real. In the limits of small and large values of the radiation parameter Γ, the following values are obtained:

$$\left.\begin{aligned} &\Gamma \ll 1: \quad \sigma_0 \to \Gamma, \quad \sigma_r \to ((\gamma-1)/2)\,\Gamma, \quad \sigma_i \to 1, \\ &\Gamma \gg 1: \quad \sigma_0 \to \gamma\Gamma, \quad \sigma_r \to ((\gamma-1)/2\gamma^2)\,(1/\Gamma), \quad \sigma_i \to \gamma^{-\frac{1}{2}}. \end{aligned}\right\} \tag{9}$$

The roots σ_0, σ_r, and σ_i vary smoothly between the above limits, as shown in figure 2 for $\gamma = \frac{5}{3}$.

Previous studies of this time-damped case were concerned only with the analysis of the three roots (decay frequencies) of the characteristic equation. In the remainder of § 2 we shall proceed one step further by calculating the amplitudes of the terms involving the three decay frequencies, i.e. we shall carry out the complete solution for the decay of initial sinusoidal perturbations in temperature, velocity and pressure.

The total solution for the radiative decay of a sinusoidal perturbation consists

of three exponential terms involving the three decay frequencies σ_0, σ_+ and σ_-, respectively. Accordingly, the solution for the potential is given by

$$\phi = \mathrm{Re}\left\{\frac{a_0}{k}(c_0 e^{-\sigma_0 k a_0 t} + c_+ e^{-\sigma_+ k a_0 t} + c_- e^{-\sigma_- k a_0 t})\, e^{i\mathbf{k}\cdot\mathbf{s}}\right\}, \tag{10}$$

where Re denotes the real part. The complex non-dimensional amplitudes c_0 and $c_\pm$ are determined below in terms of the radiation parameter Γ and the

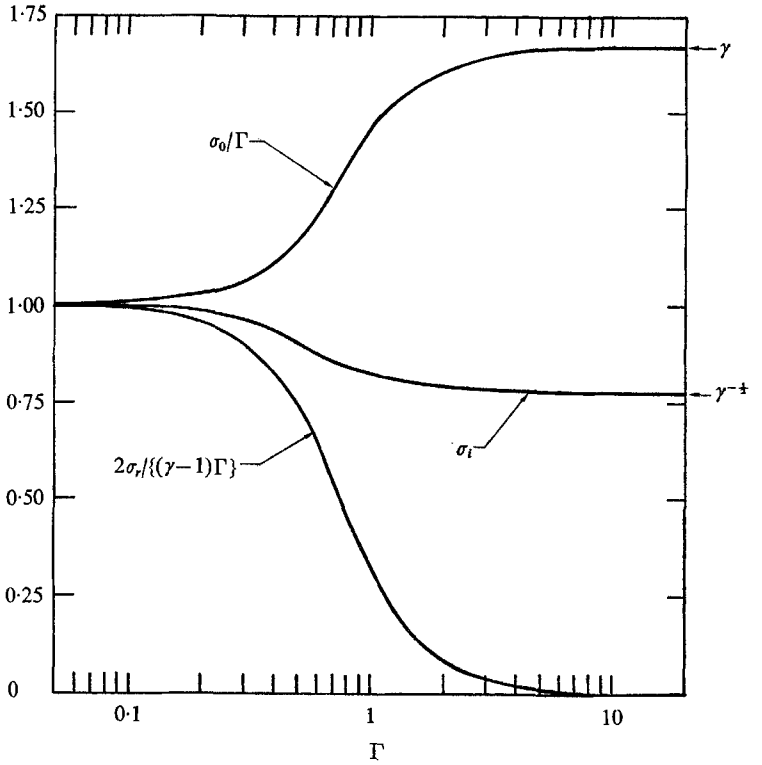

FIGURE 2. Real and imaginary decay frequencies as functions of the radiation parameter Γ; computed for $\gamma = \frac{5}{3}$.

initial conditions. Substitution of (10) into (3) yields the following relations for the perturbation velocity u' in the $\mathbf{k}$ direction and the perturbation pressure p':

$$\frac{u'}{a_0} = \mathrm{Re}\{i(c_0 e^{-\sigma_0 k a_0 t} + c_+ e^{-\sigma_+ k a_0 t} + c_- e^{-\sigma_- k a_0 t})\, e^{i\mathbf{k}\cdot\mathbf{s}}\}, \tag{11}$$

$$\frac{p'}{p_0} = \mathrm{Re}\{\gamma(\sigma_0 c_0 e^{-\sigma_0 k a_0 t} + \sigma_+ c_+ e^{-\sigma_+ k a_0 t} + \sigma_- c_- e^{-\sigma_- k a_0 t})\, e^{i\mathbf{k}\cdot\mathbf{s}}\}. \tag{12}$$

The temperature perturbation is represented by

$$\frac{T'}{T_0} = \mathrm{Re}\{(b_0 e^{-\sigma_0 k a_0 t} + b_+ e^{-\sigma_+ k a_0 t} + b_- e^{-\sigma_- k a_0 t})\, e^{i\mathbf{k}\cdot\mathbf{s}}\}, \tag{13}$$

where the amplitudes b_0 and $b_\pm$ are related to the c_0 and $c_\pm$ amplitudes by means of (2):

$$b_0 = \left(\frac{1}{\sigma_0} + \gamma\sigma_0\right) c_0; \quad b_\pm = \left(\frac{1}{\sigma_\pm} + \gamma\sigma_\pm\right) c_\pm. \tag{14}$$

For the initial conditions we consider the following sinusoidal disturbances:

$$\left.\begin{aligned} \frac{T'(\mathbf{s},0)}{T_0} &= \mathrm{Re}\{(b_0+b_++b_-)\,e^{i\mathbf{k}\cdot\mathbf{s}}\} = \mathrm{Re}\{\Delta_1 e^{i\mathbf{k}\cdot\mathbf{s}}\},\\ \frac{u'(\mathbf{s},0)}{a_0} &= \mathrm{Re}\{i(c_0+c_++c_-)\,e^{i\mathbf{k}\cdot\mathbf{s}}\} = \mathrm{Re}\{\Delta_2 e^{i\mathbf{k}\cdot\mathbf{s}}\},\\ \frac{p'(\mathbf{s},0)}{p_0} &= \mathrm{Re}\{\gamma(\sigma_0 c_0+\sigma_+ c_++\sigma_- c_-)\,e^{i\mathbf{k}\cdot\mathbf{s}}\} = \mathrm{Re}\{\Delta_3 e^{i\mathbf{k}\cdot\mathbf{s}}\}, \end{aligned}\right\} \tag{15}$$

where the amplitudes Δ_j may be complex to allow for arbitrary phase differences between the initial sinusoidal disturbances. Perturbations for different wave-numbers $\mathbf{k}$ may be superposed to obtain solutions for arbitrary initial disturbances (see § 3).

Equations (14) and (15) may be solved for the perturbation amplitudes, expressed in terms of the roots σ_0, σ_r and σ_i,

$$\left.\begin{aligned} c_0 &= \left(\frac{1}{\sigma_0}+\gamma\sigma_0\right)^{-1} b_0 = \frac{(\sigma_r^2+\sigma_i^2)\,\Delta_1 + 2i\sigma_r\Delta_2 + [1-\gamma(\sigma_r^2+\sigma_i^2)]\,\gamma^{-1}\Delta_3}{[(\sigma_0-2\sigma_r)+(1/\sigma_0)\,(\sigma_r^2+\sigma_i^2)]},\\ c_\pm &= -\frac{1}{2}\left[1 \mp i\left(\frac{\sigma_0-\sigma_r}{\sigma_i}\right)\right] c_0 \mp \frac{1}{2\sigma_i}\,[(\sigma_r \pm i\sigma_i)\,\Delta_2 + i\gamma^{-1}\Delta_3],\\ b_\pm &= \left\{\frac{[1+\gamma(\sigma_r^2+\sigma_i^2)]\,\sigma_r \mp i[1-\gamma(\sigma_r^2+\sigma_i^2)]\,\sigma_i}{(\sigma_r^2+\sigma_i^2)\,\{(1/\sigma_0)+\gamma\sigma_0\}}\right\}\left(\frac{c_\pm}{c_0}\right). \end{aligned}\right\} \tag{16}$$

The radiative decay of a sinusoidal disturbance is thus given by (11), (12), (13) and (16), expressed in terms of the roots σ_0, σ_r and σ_i, which may be determined from the cubic equation (6) for any value of the radiation parameter Γ.

For the limiting values of σ_0, σ_r and σ_i given in (9), the following solutions are obtained:

$\Gamma \ll 1$:

$$\left.\begin{aligned} \frac{T'}{T_0} &\to \mathrm{Re}\left\{\left([\Delta_1-(1-\gamma^{-1})\,\Delta_3]\exp(-\Gamma k a_0 t)\right.\right.\\ &\qquad +[(1-\gamma^{-1})\,\Delta_3\cos(ka_0t)+i(\gamma-1)\,\Delta_2\sin(ka_0t)]\\ &\qquad\qquad \left.\left.\times\exp\left[-\left(\frac{\gamma-1}{2}\right)\Gamma k a_0 t\right]\right)\exp(i\mathbf{k}\cdot\mathbf{s})\right\},\\ \frac{u'}{a_0} &\to \mathrm{Re}\left\{[\Delta_2\cos(ka_0t)-i\gamma^{-1}\Delta_3\sin(ka_0t)]\right.\\ &\qquad\qquad \left.\times\exp\left[-\left(\frac{\gamma-1}{2}\right)\Gamma k a_0 t\right]\exp(i\mathbf{k}\cdot\mathbf{s})\right\},\\ \frac{p'}{p_0} &\to \mathrm{Re}\left\{[\Delta_3\cos(ka_0t)-i\gamma\Delta_2\sin(ka_0t)]\exp\left[-\left(\frac{\gamma-1}{2}\right)\Gamma k a_0 t\right]\exp(i\mathbf{k}\cdot\mathbf{s})\right\}. \end{aligned}\right\} \tag{17}$$

$\Gamma \gg 1$:

$$\left.\begin{aligned}
&\frac{T'}{T_0} \to \mathrm{Re}\{\Delta_1 \exp(-\gamma\Gamma k a_0 t)\exp(i\mathbf{k}.\mathbf{s})\},\\
&\frac{u'}{a_0} \to \mathrm{Re}\left\{[\Delta_2 \cos(\gamma^{-\frac{1}{2}} k a_0 t) + i\gamma^{-\frac{1}{2}}(\Delta_1 - \Delta_3)\sin(\gamma^{-\frac{1}{2}} k a_0 t)]\right.\\
&\qquad\qquad \left.\times \exp\left[-\left(\frac{\gamma-1}{2\gamma^2}\right)\frac{k a_0 t}{\Gamma}\right]\exp(i\mathbf{k}.\mathbf{s})\right\},\\
&\frac{p'}{p_0} \to \mathrm{Re}\left\{\left(\Delta_1 \exp(-\gamma\Gamma k a_0 t) + [(\Delta_3 - \Delta_1)\cos(\gamma^{-\frac{1}{2}} k a_0 t) - i\gamma^{\frac{1}{2}}\Delta_2 \sin(\gamma^{-\frac{1}{2}} k a_0 t)]\right.\right.\\
&\qquad\qquad \left.\left.\times \exp\left[-\left(\frac{\gamma-1}{2\gamma^2}\right)\frac{k a_0 t}{\Gamma}\right]\right)\exp(i\mathbf{k}.\mathbf{s})\right\}.
\end{aligned}\right\} \tag{18}$$

In (17) and (18) the omitted terms are of order $\Gamma\Delta_i$ and Δ_i/Γ, respectively. For the case of no initial velocity or pressure perturbations, (17) and (18) represent constant-density and constant-pressure cooling, respectively. For planetary atmospheres Γ is much less than unity (see e.g. Gille 1968). On the other hand, Γ can be of order unity in stellar atmospheres. Also, engineering applications or laboratory experiments can involve high temperatures with corresponding Γ values up to unity or greater.

The recovery of the constant density solution $\Gamma \gg 1$ was to be expected since for a sufficiently large cooling rate the gas does not have time to move during the cooling period. In this connexion we note that (18) gives a cooling time which is of order $1/\Gamma$ shorter than the period of the velocity and pressure oscillations. For the $\Gamma \ll 1$ case the cooling time is much longer (order $1/\Gamma$) than the period of velocity and pressure oscillations. From (18) for $\Gamma \gg 1$ we also see that pressure and velocity perturbations of order Δ_1 are induced by the initial temperature profile of amplitude Δ_1. These induced pressures and velocities were negligible in the $\Gamma \ll 1$ case since they were of order $\Gamma\Delta_1$.

For intermediate values of Γ all three roots σ_0, σ_+ and σ_- will contribute to the temperature cooling. Again considering an initial perturbation only in the temperature, the amplitude b_0 is given by the first of (16) with $\Delta_2 = \Delta_3 = 0$, and the relative amplitudes of the terms containing $\sigma_\pm$ are given by

$$b_\pm/b_0 = \beta_r \pm i\beta_i, \tag{19}$$

where

$$\left.\begin{aligned}
\beta_r &= \frac{\sigma_0[1-\gamma(\sigma_r^2+\sigma_i^2)] - 2\sigma_r}{2(\sigma_r^2+\sigma_i^2)\{(1/\sigma_0)+\gamma\sigma_0\}},\\
\beta_i &= \frac{\sigma_r(\sigma_0-\sigma_r)[1+\gamma(\sigma_r^2+\sigma_i^2)] + \sigma_i^2[1-\gamma(\sigma_r^2+\sigma_i^2)]}{2\sigma_i(\sigma_r^2+\sigma_i^2)\{(1/\sigma_0)+\gamma\sigma_0\}}.
\end{aligned}\right\} \tag{20}$$

The factors β_r and β_i are plotted in figure 3. For $\Delta_2 = \Delta_3 = 0$, (16) give

$$c_\pm/c_0 = \gamma_r \pm i\gamma_i,$$

where

$$\gamma_r = -\tfrac{1}{2} \quad \text{and} \quad \gamma_i = (\sigma_0 - \sigma_r)/2\sigma_i.$$

For b_0 real, the solutions (11) through (13) reduce to

$$\left.\begin{aligned} T'/T_0 &= b_0(e^{-\sigma_0 k a_0 t} + 2e^{-\sigma_r k a_0 t}[\beta_r \cos(\sigma_i k a_0 t) + \beta_i \sin(\sigma_i k a_0 t)])\cos \mathbf{k}.\mathbf{s}, \\ u'/a_0 &= -c_0(e^{-\sigma_0 k a_0 t} + 2e^{-\sigma_r k a_0 t}[\gamma_r \cos(\sigma_i k a_0 t) + \gamma_i \sin(\sigma_i k a_0 t)])\sin \mathbf{k}.\mathbf{s}, \\ p'/p_0 &= \gamma c_0(\sigma_0 e^{-\sigma_0 k a_0 t} + 2e^{-\sigma_r k a_0 t}[(\sigma_r \gamma_r - \sigma_i \gamma_i)\cos(\sigma_i k a_0 t) \\ &\qquad + (\sigma_i \gamma_r + \sigma_r \gamma_i)\sin(\sigma_i k a_0 t)])\cos \mathbf{k}.\mathbf{s}, \end{aligned}\right\} \quad (21)$$

where $c_0 = \sigma_0 b_0/(1+\gamma\sigma_0^2)$.

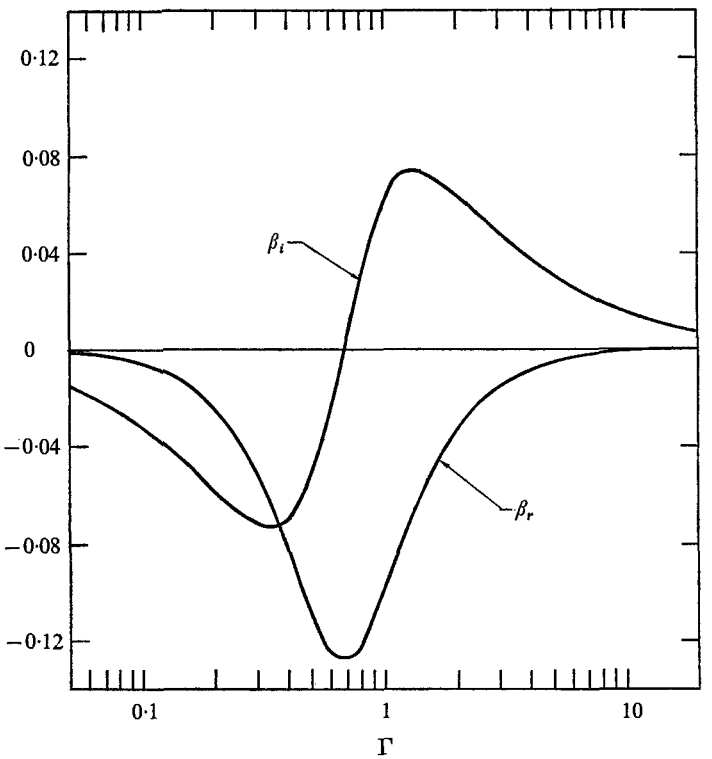

FIGURE 3. Temperature decay coefficients as functions of the radiation parameter Γ; computed for $\gamma = \frac{5}{3}$.

3. Radiative decay of step temperature profiles

The sinusoidal perturbations of § 2 may be superposed to yield the solution for the decay of any initial temperature, velocity, and pressure profiles in a radiating gas. In this section we obtain solutions for the decay of planar, cylindrical and spherical step temperature profiles. Sample calculations are carried out for planar step profiles in a gray gas.

Consider the decay of a planar step temperature profile, i.e. an initial temperature perturbation which has the constant value $T_0\Delta$ between $-x_0$ and $+x_0$,

and is zero elsewhere. Superposition of the solutions (21) with $\mathbf{k}.\mathbf{s} = kx$ gives

$$\left.\begin{aligned} \frac{T'(x,t)}{T_0} &= \int_0^\infty \bar{T}(k,t)\cos kx\,dk, \\ \frac{u'(x,t)}{a_0} &= \int_0^\infty \bar{u}(k,t)\sin kx\,dk, \\ \frac{p'(x,t)}{p_0} &= \int_0^\infty \bar{p}(k,t)\cos kx\,dk, \end{aligned}\right\} \tag{22}$$

where $\bar{T}(k,t)$, $\bar{u}(k,t)$ and $\bar{p}(k,t)$ correspond to the right-hand sides of (21) exclusive of the $\cos\mathbf{k}.\mathbf{s}$ and $\sin\mathbf{k}.\mathbf{s}$ factors. At the initial time, $\bar{T}(k,0) = b_0(1+2\beta_r)$. Application of Fourier cosine transform theory to the initial temperature profile yields the following expression for $b_0(k)$

$$\begin{aligned} b_0(k) &= (1+2\beta_r)^{-1}\bar{T}(k,0) = (1+2\beta_r)^{-1}\frac{2}{\pi}\int_0^\infty \frac{T'(x,0)}{T_0}\cos kx\,dx \\ &= \frac{2\Delta\sin kx_0}{\pi k(1+2\beta_r)}. \end{aligned} \tag{23}$$

Substitution of $b_0(k)$ into (22) gives the following solution expressed in terms of the non-dimensional time $\tau \equiv \alpha_0 a_0 t$ and optical distance $\xi \equiv \alpha_0 x$, with $\xi_0 \equiv \alpha_0 x_0$:

$$\frac{T'(\xi,\tau)}{T_0\Delta} = \frac{2}{\pi}\int_0^\infty \{e^{-\sigma_0\kappa\tau} + 2e^{-\sigma_r\kappa\tau}[\beta_r\cos(\sigma_i\kappa\tau) + \beta_i\sin(\sigma_i\kappa\tau)]\}\frac{\cos\kappa\xi\sin\kappa\xi_0}{(1+2\beta_r)\kappa}\,d\kappa, \tag{24}$$

$$\frac{u'(\xi,\tau)}{a_0\Delta} = -\frac{2}{\pi}\int_0^\infty \left\{e^{-\sigma_0\kappa\tau} - e^{-\sigma_r\kappa\tau}\left[\cos(\sigma_i\kappa\tau) - \left(\frac{\sigma_0-\sigma_r}{\sigma_i}\right)\sin(\sigma_i\kappa\tau)\right]\right\} \times \frac{\sin\kappa\xi\sin\kappa\xi_0}{(1+2\beta_r)\kappa}\left(\frac{\sigma_0}{1+\gamma\sigma_0^2}\right)d\kappa, \tag{25}$$

$$\frac{p'(\xi,\tau)}{\gamma p_0\Delta} = \frac{2}{\pi}\int_0^\infty \left\{e^{-\sigma_0\kappa\tau} - e^{-\sigma_r\kappa\tau}\left[\cos(\sigma_i\kappa\tau) + \left(\frac{\sigma_r^2+\sigma_i^2-\sigma_0\sigma_r}{\sigma_0\sigma_i}\right)\sin(\sigma_i\kappa\tau)\right]\right\} \times \frac{\cos\kappa\xi\sin\kappa\xi_0}{(1+2\beta_r)\kappa}\left(\frac{\sigma_0^2}{1+\gamma\sigma_0^2}\right)d\kappa. \tag{26}$$

The β factors appearing in (24) are given by (20) in terms of the σ's, which are determined from the cubic equation (6) involving the radiation parameter Γ. For a gray gas $\Gamma(\kappa)$ is given by (8), whereas for a non-gray gas the appropriate Γ function may be obtained from Goody (1964), Sasamori & London (1966), or Gille (1968).

Equations (24) through (26) contain two independent parameters, Bo and ξ_0. In the constant-pressure and constant-density limits, perturbations arise only from the σ_0 root, which becomes inversely proportional to Bo. For these limiting cases, the Boltzmann number may be absorbed in the time variable

$$\tilde{\tau} \equiv (16/Bo)\tau = (16/Bo)\alpha_0 a_0 t,$$

which is proportional to the total amount of energy emitted up to time t. In this paper we consider all three σ roots, which depend on Bo in a complicated manner;

therefore the solutions expressed in terms of $\tilde{\tau}$ will not be entirely independent of Bo.

Reference to the integrals (24) through (26) shows that we cannot combine Bo and ξ_0 into a single parameter because the component sinusoidal functions are weighted differently for different times and positions. As a result, the profile shapes depend on the optical width of the initial step. Also, the step profiles decay through a series of non-similar profiles, i.e. the profile shapes vary with time. These results may be contrasted with the previous results for pure sinusoidal profiles, which depend only on one radiation parameter, and retain their original shape throughout the decay period.

Although the solutions depend on both ξ and ξ_0, the term $2\cos\kappa\xi\sin\kappa\xi_0$ appearing in (24) may be written as $\sin\kappa(\xi_0+\xi)+\sin\kappa(\xi_0-\xi)$; thus the temperature perturbation may be expressed as the sum of two contributions, each depending only on the optical distance from a discontinuity. Considering the solution near the edge of a semi-infinite profile ($\xi_0\to\infty$ but $\hat{\xi}\equiv\xi-\xi_0$ finite), the term involving $\sin\kappa(\xi_0+\xi)$ integrates to give a contribution of $\frac{1}{2}$ to $T'/T_0\Delta$, with the remaining contribution depending only on $\hat{\xi}$. It is concluded that calculations need be carried out only for the semi-infinite profile, since the solution for a profile of total width $2\xi_0$ may be obtained by adding the temperature perturbations at the positions $\hat{\xi}=\xi_0+\xi$ and $\hat{\xi}=\xi_0-\xi$ on the semi-infinite profile and subtracting unity. This last result simply reflects the fact that a finite step may be constructed from two semi-infinite steps.

Several limiting forms of (24) may be considered. When $Bo\to\infty$, but $\tilde{\tau}\equiv(16/Bo)\tau$ remaining finite, then $\Gamma\to 0$, yielding $\beta_i\to\beta_r\to 0$ and $\sigma_0\to\Gamma$. Therefore,

$$\frac{T'(\xi,\tau)}{T_0\Delta}\to\frac{2}{\pi}\int_0^\infty[\exp\{-\tilde{\tau}(1-\kappa^{-1}\tan^{-1}\kappa)\}]\frac{\cos\kappa\xi\sin\kappa\xi_0}{\kappa}d\kappa. \tag{27}$$

The constant pressure solution (27) is the same as that for free mixing flow given by Sforza & Porter (1968) if the heat conduction is neglected in their (33).

In the optically thin limit ($\xi_0\ll 1$), the dominant contribution to the integral in (27) arises when $\kappa\gg 1$, therefore

$$\left.\begin{aligned}\frac{T'(\xi,\tau)}{T_0\Delta}&\to e^{-\tilde{\tau}}\quad\text{for}\quad|\xi|<\xi_0,\\ &\to 0\quad\text{for}\quad|\xi|>\xi_0.\end{aligned}\right\} \tag{28}$$

The solution (28) may be obtained directly from the energy equation if constant pressure is assumed and if the linearized flux divergence expression for optically thin emission is used, i.e. $\partial q_j^{R'}/\partial x_j=16\sigma T_0^3T'$ for $|\xi|<\xi_0$ and zero for $|\xi|>\xi_0$.

In the optically thick limit ($\xi_0\gg 1$), the integral in (27) may be evaluated by setting $\kappa\ll 1$. Thus $(1-\kappa^{-1}\tan^{-1}\kappa)\to\kappa^2/3$, and

$$\frac{T'(\xi,\tau)}{T_0\Delta}\to\frac{1}{2}\left[\operatorname{erf}\left\{\left(\frac{3}{4\tilde{\tau}}\right)^{\frac{1}{2}}(\xi_0+\xi)\right\}+\operatorname{erf}\left\{\left(\frac{3}{4\tilde{\tau}}\right)^{\frac{1}{2}}(\xi_0-\xi)\right\}\right], \tag{29}$$

where erf denotes the error function. Equation (29) is the same as the heat conduction solution given by Carslaw & Jaeger (1959), if we define an effective thermal diffusivity equal to $16\alpha_0/3Bo\alpha_0$. This result was to be expected, since use

of the Rosseland diffusion approximation for the flux in an optically thick medium reduces the constant-pressure energy equation to the heat conduction equation with this same effective thermal diffusivity. This analysis for an optically thick medium will not be valid at very small times, when a temperature discontinuity still exists.

Equations (27) through (29) will give accurate profiles when $\Gamma(\kappa) \ll 1$ for the range of κ values providing the dominant contribution to the κ-integral. It will

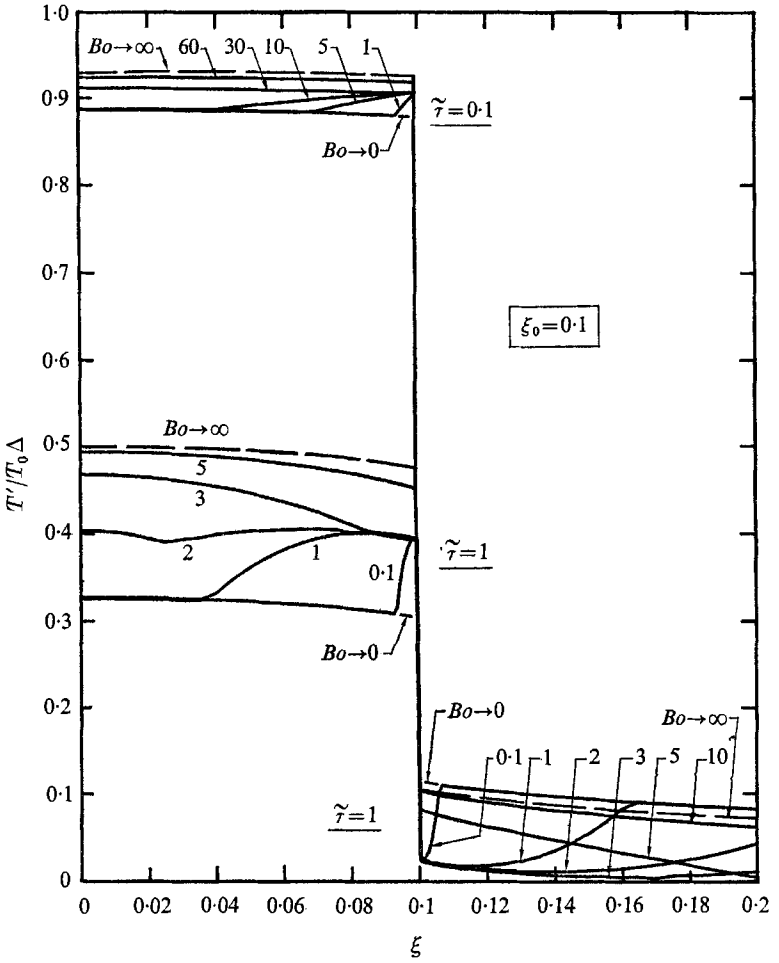

FIGURE 4. Temperature perturbation profiles for the decay of initial planar step profiles with total optical thicknesses $2\xi_0 = 0{\cdot}2$. Computed for a gray gas with $\gamma = \frac{5}{3}$.

be shown later that these constant-pressure formulas are accurate not only for $Bo \gg 1$, but also for the final cooling stages of gases with Bo of order unity or smaller. Substitution of $\gamma\tilde{\tau}$ for $\tilde{\tau}$ in (27) through (29) yields constant-density solutions, which will be applicable for $Bo \to 0$, and also for the early cooling stages of gases with Bo values up to about 20.

Numerical evaluation of the integral in (24) for a gray gas provides the tempera-

ture perturbation profiles shown in figures 4–6. The solid curves were plotted by the computer, and the dashed curves were drawn in by hand from calculations utilizing the limiting form (27). The curves should be accurate to a fraction of 1 % of the full scale value; however, since only 50 to 100 points were computed for each curve, some sharp corners and small wiggles are the result of computer-plotting. The rapid variations or waves in the temperature profiles are produced by the gas motion, as discussed below in connexion with figures 6–8.

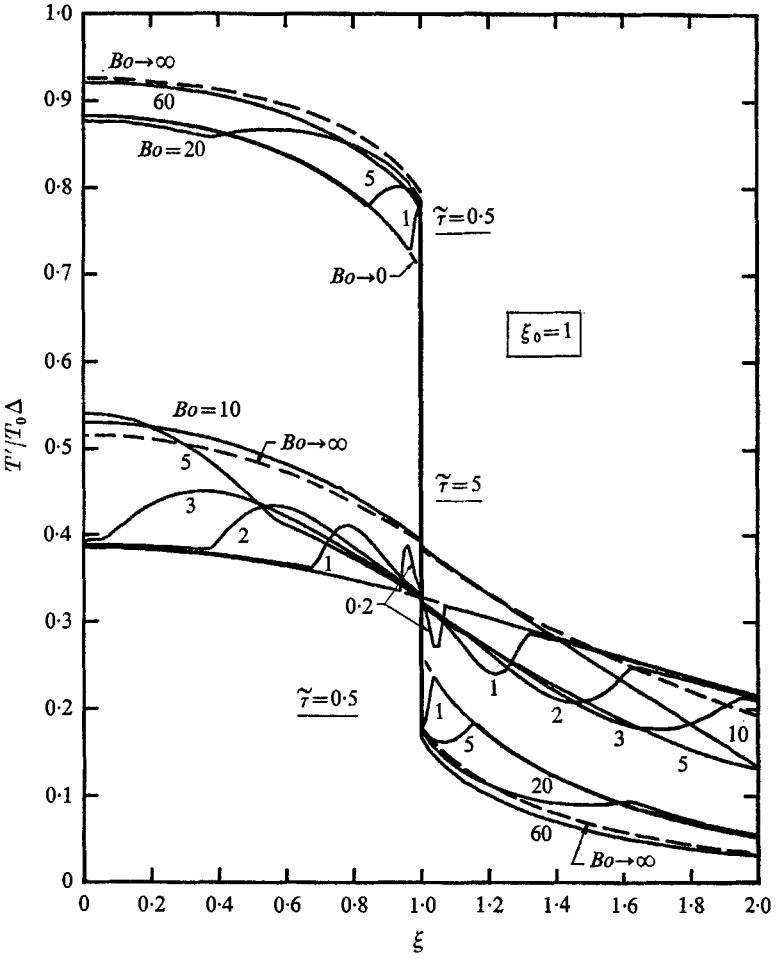

FIGURE 5. Temperature perturbation profiles for the decay of initial planar step profiles with total optical thicknesses $2\xi_0 = 2$. Computed for a gray gas with $\gamma = \frac{5}{3}$.

Figure 4 presents perturbation temperature profiles for the relatively thin initial profile of optical thickness $2\xi_0 = 0{\cdot}2$. Curves are shown for the non-dimensional times $\tilde{\tau} = 0{\cdot}1$ and 1, with the curves for $\xi > \xi_0$ at $\tilde{\tau} = 0{\cdot}1$ being omitted since they lie near zero and would add confusion to the figure. Because there is about 20 % absorption within the profile width $2\xi_0$, the temperature decrease at constant pressure ($Bo \to \infty$) is only about 70 to 80 % of the decrease

given by (28). It is noted that the decaying profiles remain nearly flat, as they would for an optically thin gas. The transition from the constant pressure cooling for small radiative transfer (large Bo) to constant density cooling for large radiative transfer (small Bo) is clearly illustrated in figure 4. A gas characterized by an intermediate Bo value will progress in time from constant density cooling to constant pressure cooling.

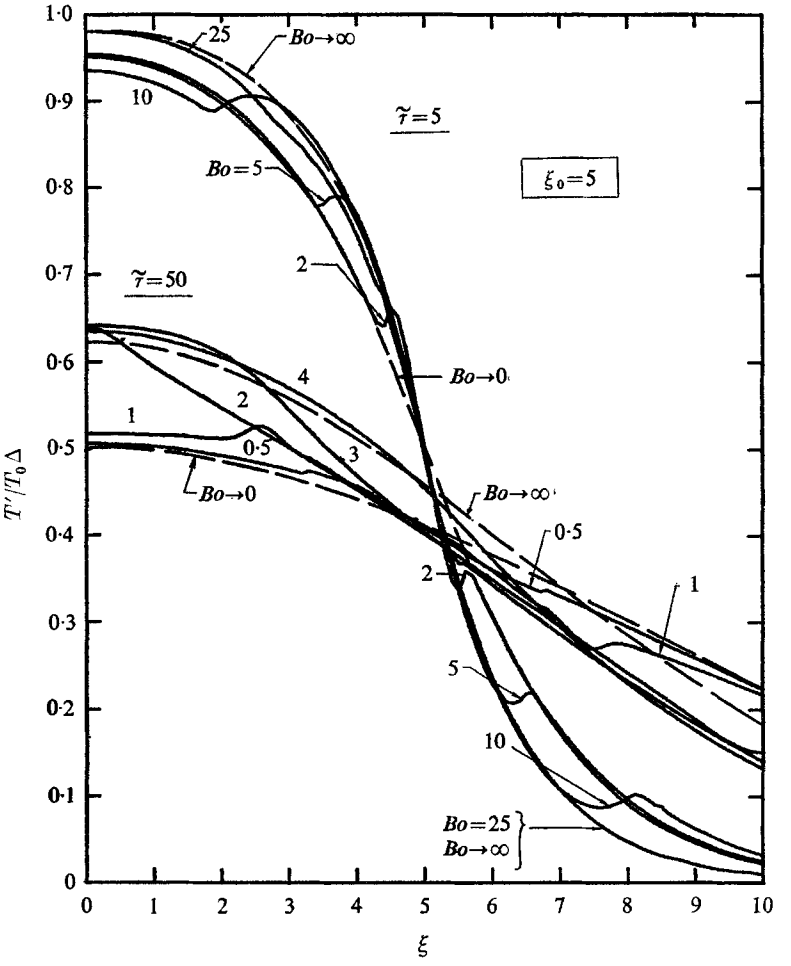

FIGURE 6. Temperature perturbation profiles for the decay of initial planar step profiles with total optical thicknesses $2\xi_0 = 10$. Computed for a gray gas with $\gamma = \frac{5}{3}$.

Temperature profiles for the intermediate profile width $2\xi_0 = 2$ are shown in figure 5. Comparison with figure 4 shows that the increased absorption results in greater profile curvature, as well as a slower temperature decay with time $\tilde{\tau}$. The gas in the region $\xi > \xi_0$ becomes appreciably heated, resulting in nearly continuous profiles at $\tilde{\tau} = 5$.

For the relatively thick profile $2\xi_0 = 10$ shown in figure 6, the profiles are continuous for the times $\tilde{\tau}$ shown. If (29) is used to compute the constant pressure

($Bo \to \infty$) curves shown in figure 6, errors of less than five and one percent of full scale are obtained for the times $\tilde{\tau} = 5$ and 50, respectively. (Similar accuracy holds for the constant density case.)

In order to further illustrate the decay of perturbations, the integrals appearing in (24) through (26) were numerically evaluated for the intermediate Boltzmann number $Bo = 5$. Figure 7 shows the decay of the initial step temperature

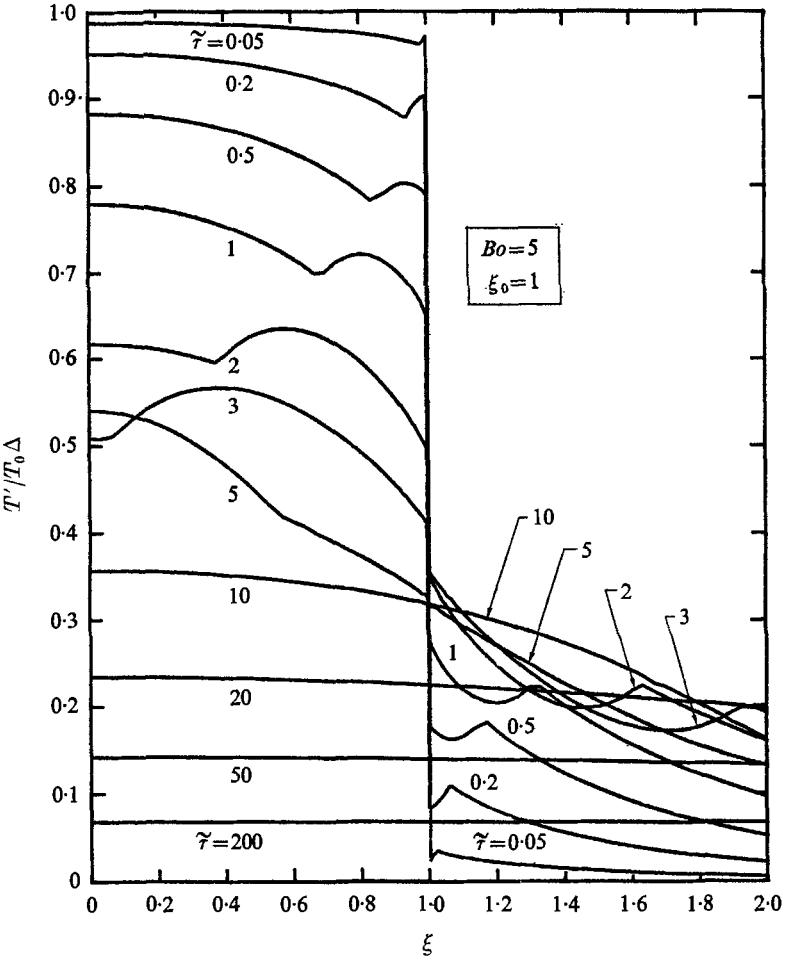

FIGURE 7. Temperature perturbation profiles during the decay of an initial planar step temperature profile of total optical thickness $2\xi_0 = 2$. Computed for a gray gas with $Bo = 5$ and $\gamma = \frac{5}{3}$.

perturbation, with the development and decay of the velocity and pressure perturbations being shown in figures 8 and 9, respectively. Radiative transfer produces nearly constant density cooling and heating at very early times, before the gas has had time to move. The cooling in the region $\xi < \xi_0$ and the heating in the region $\xi > \xi_0$ sets up a pressure perturbation which varies rapidly in the vicinity of the temperature discontinuity. This large positive pressure gradient

produces a negative (towards $\xi = 0$) velocity pulse. In turn, as the gas motion starts to equilibrate the pressure, the temperature perturbations near the discontinuity at $\xi = \xi_0$ will start to approach the values appropriate for constant pressure cooling and heating. Thus temperature pulses appear on either side of the discontinuity in figure 7.

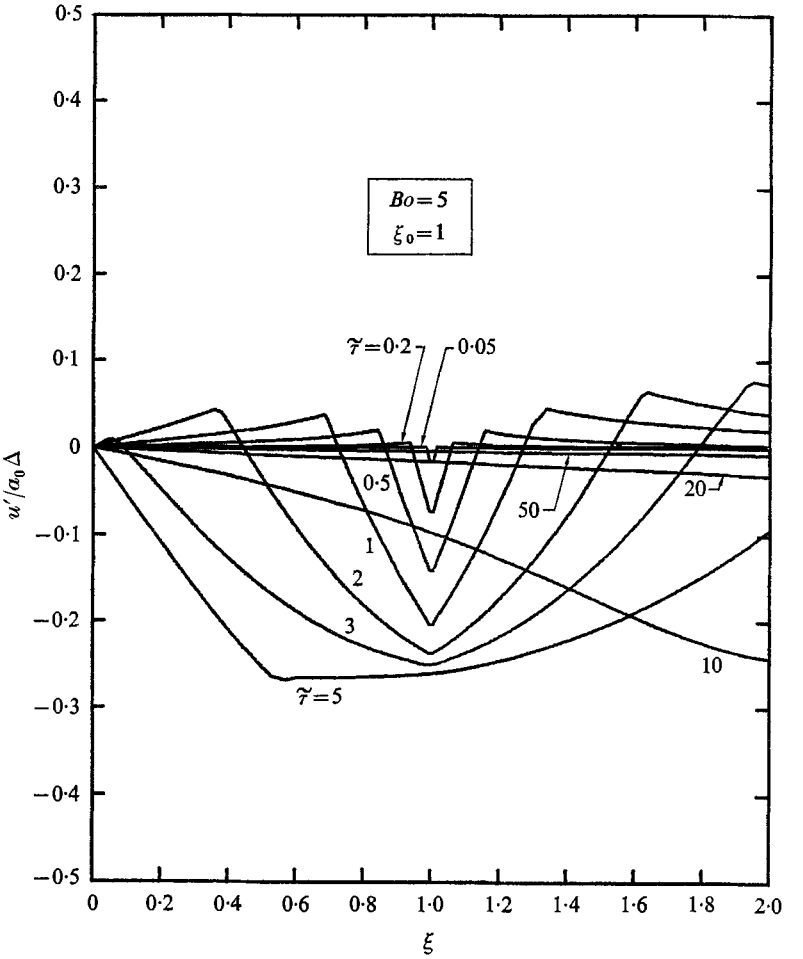

FIGURE 8. Velocity perturbation profiles during the decay of an initial planar step temperature profile of total optical thickness $2\xi_0 = 2$. Computed for a gray gas with $Bo = 5$ and $\gamma = \frac{5}{3}$.

As time progresses the pressure and velocity perturbations increase and spread out to farther distances from ξ_0. The velocity and pressure distributions produce a spreading of the temperature pulses; i.e. the gasdynamics produces heating and cooling waves travelling inward and outward, respectively, from the discontinuity at speeds approximately equal to the acoustic velocity a_0. These waves of gasdynamic origin may be contrasted with the purely thermal cooling waves produced in the non-linear problem by the temperature dependence of absorption in air; see Zel'dovich & Raizer (1967).

After the perturbation pulses reach $\xi = 0$, the accumulation of mass results in a pressure increase in the core region $\xi < \xi_0$. On the other hand, mass loss and reradiation decrease the pressure in the portion $\xi_0 < \xi < 2\xi_0$ of the outer region shown in figure 9. The pressure increase near $\xi = 0$ reduces the inward gas flow in the core, whereas the progression of the outward pressure wave leads to appreciable inward velocities at large distances (note the $\tilde{\tau} = 10$ curve of figure 8).

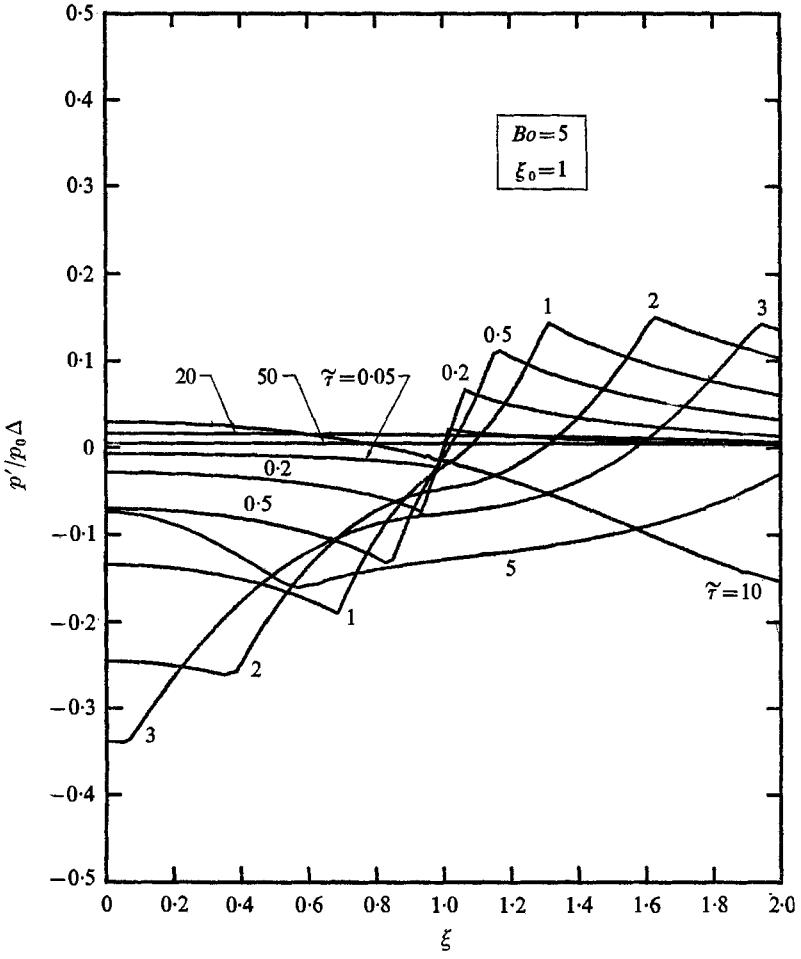

FIGURE 9. Pressure perturbation profiles during the decay of an initial planar step temperature profile of total optical thickness $2\xi_0 = 2$. Computed for a gray gas with $Bo = 5$ and $\gamma = \frac{5}{3}$.

The reduction of the negative pressure perturbation in the core results in a reflected temperature wave consisting of temperature perturbations which are closer to the constant pressure values (cf. figures 5 and 7). This reflected wave represents the wave originating from the far discontinuity at $\xi = -\xi_0$. As shown in figure 7, the local temperature actually increases during the non-dimensional time period $\tilde{\tau} \simeq 3$ to 5 when the waves are passing through the profile centre.

At later times the pressure and velocity perturbations decay to zero, with the temperature perturbations decaying at nearly constant pressure.

The gasdynamic transition from constant-density to constant-pressure cooling described above corresponds to a linearized analogue of the following sequence of events occurring after a strong explosion: radiative cooling and diffusion at constant density, followed by the formation and propagation of a blast wave, after which radiative cooling occurs at nearly constant pressure; see e.g. Zel'dovich & Raizer (1967). For our linearized problem, reference to figures 4–6 shows that gasdynamic waves and transitions from constant-density to constant-pressure cooling will occur for a broad range of intermediate and small Boltzmann numbers. Since the waves will travel at roughly the sound speed a_0, waves generated at the temperature discontinuities will reach the profile centre at approximately the time $t^* = x_0/a_0$, which gives the non-dimensional transition times $\tau^* = \xi_0$ and $\tilde{\tau}^* = (16/Bo)\,\xi_0$. This expression for $\tilde{\tau}^*$ correlates very well with arrival of the wave at the profile centre, at which time the temperature curve is very nearly midway between the constant-density and constant-pressure curves; see figures 4–7.

The transition time $\tilde{\tau}^*$ may be compared with the time $\tilde{\tau}_c$ required for the temperature perturbation at the profile centre to decay to half its initial value. Equations (28) and (29) give $\tilde{\tau}_c$ values of approximately 0·7 and $3\xi_0^2$ for the optically thin and thick limits, respectively; therefore, $\tilde{\tau}^*/\tilde{\tau}_c \simeq 24\xi_0/Bo$ for $\xi_0 \ll 1$ and $\tilde{\tau}^*/\tilde{\tau}_c \simeq 16/3\xi_0 Bo$ for $\xi_0 \gg 1$. Accordingly, the transition will occur before the final stages of cooling for a relatively wide range of Bo values, with this range becoming wider as ξ_0 increases or decreases away from order unity.

The behaviour of the step profile solutions may be discussed in terms of a superposition of sinusoidal waves. When Bo is greater than about 30, $\Gamma(\kappa) \lesssim 0{\cdot}1$ and the sinusoidal solutions for all κ values decay at nearly constant pressure; therefore, the superposed step profile decays at nearly constant pressure. For a given intermediate or small value of Bo, a sufficiently large value of τ may be chosen so that the exponentials in (24) are negligibly small except for κ so small that $\Gamma(\kappa) \ll 1$; thus the constant-pressure solution is applicable at sufficiently large times τ.

The induced non-dimensional velocity and pressure perturbations are appreciable for the $Bo = 5$ case shown in figures 8 and 9. These perturbations increase with decreasing Bo. As the strong radiation limit ($Bo \to 0$) is approached, $|p'/\gamma p_0 \Delta|$ and $|u'/a_0 \Delta|$ approach the maximum values γ^{-1} and $\gamma^{-\frac{1}{2}}$, respectively, with oscillations and decay of these perturbations occurring over progressively longer times (cf. (18) for the sinusoidal case). As given by the equation of state, the non-dimensional density perturbation ρ'/ρ_0 is equal to p'/p_0 minus T'/T_0. Thus, for weak radiation ($Bo \gg 1$) the density perturbation follows the temperature perturbation, whereas for strong radiation ($Bo \ll 1$), the density will remain nearly constant during the cooling period, and will oscillate and decay over longer periods along with the induced pressure perturbation.

The calculations presented in this section involve several simplifying assumptions and arbitrary conditions. However, these calculations should qualitatively describe important features present for other situations.

A non-gray gas could be considered by the use of the appropriate non-gray radiation parameter $\Gamma(k)$ in the above calculational procedure. Since $\Gamma(k)$ has a broader maximum for a non-gray gas (see e.g. Gille 1968), one would expect that the constant-density régime might be more important than for a gray gas; however, the general features of the cooling and gasdynamics should be the same.

Specific calculations were carried out for the case of no initial perturbations in the pressure or gas velocity. Of course, for a particular application the appropriate initial conditions are determined by the manner in which the initial perturbations are established. In this general study we could easily add solutions for decaying initial pressure and velocity perturbations (with no initial temperature perturbations) to the present solutions, however, a brief consideration of the problem should be sufficient to establish the general features. For example, an initial pressure perturbation consisting of a positive step profile will produce an outward expansion which will tend to counteract the inward expansion produced by the cooling of an initial step temperature perturbation. These expansions cannot entirely cancel each other since the outward expansion of the initial pressure perturbation begins immediately, whereas the inward expansion develops as the temperature profile cools. Therefore, the development of gasdynamic waves and the transition from constant-density to constant-pressure cooling (when $Bo \lesssim 20$) should be features of most cooling problems, even when initial pressure and velocity perturbations exist.

Although the calculations of this section were carried out for initial temperature profiles given by step functions, the same decay features should be exhibited by most initial temperature profiles. (The pure sinusoidal profile considered in the preceding section represents an exceptional case.) Initial temperature profiles which decrease smoothly from the centre temperature may exhibit more gradual expansion waves than do the step profiles, however, the differences are probably not great. In this regard we note that for step profiles of large optical thickness, the waves occurring at late times are induced predominantly by the cooling of relatively smooth profiles, since temperature discontinuities exist only at relatively small times for optically thick profiles.

The effect of non-planar temperature profiles may be studied by consideration of cylindrically and spherically symmetric step profiles. Superposition of sinusoidal solutions in the cylindrically symmetric case consists of integrating $\cos(\mathbf{k}.\mathbf{s}) = \cos(kr\cos\theta)$ from $\theta = -\frac{1}{2}\pi$ to $\frac{1}{2}\pi$, where θ is the angle between $\mathbf{k}$ and the vector $\mathbf{s}$ to a particular point, and $r = |\mathbf{s}|$ is the cylindrical radius. Integration gives temperature and pressure perturbations proportional to the zeroth-order Bessel function $J_0(kr)$. The velocity perturbation involves integration of $\cos\theta\sin(kr\cos\theta)$, which yields a solution proportional to the first-order Bessel function $J_1(kr)$. Of course, these elementary solutions may also be obtained (more laboriously) from the conservation and transfer equations written in cylindrical co-ordinates.

By following the procedure used for the planar case, we may determine the solution for the decay of a cylindrical step profile, i.e. for an initial temperature perturbation which has the constant value $T_0\Delta$ for $0 \leqslant r < r_0$ and zero for $r \geqslant r_0$. Integration of the elementary cylindrical solutions over wave-number k

gives (22), but with $\cos kx$ and $\sin kx$ replaced by $J_0(kr)$ and $J_1(kr)$, respectively. Evaluation of the coefficient $b_0(k)$ may be achieved by the use of the Fourier–Bessel transform,

$$b_0(k) = (1+2\beta_r)^{-1}\overline{T}(k,0) = (1+2\beta_r)^{-1}k\int_0^\infty \frac{T'(r,0)}{T_0}J_0(kr)\,r\,dr$$
$$= (1+2\beta_r)^{-1}r_0\Delta J_1(kr_0). \tag{30}$$

Use of this $b_0(k)$ gives the following solution expressed in terms of $\tau \equiv \alpha_0 a_0 t$ and $\xi = \alpha_0 r$ (with $\xi_0 \equiv \alpha_0 r_0$):

$$\frac{T'(\xi,\tau)}{T_0\Delta} = \xi_0\int_0^\infty \{e^{-\sigma_0\kappa\tau} + 2e^{-\sigma_r\kappa\tau}[\beta_r\cos(\sigma_i\kappa\tau)+\beta_i\sin(\sigma_i\kappa\tau)]\}\frac{J_0(\kappa\xi)J_1(\kappa\xi_0)}{(1+2\beta_r)}\,d\kappa, \tag{31}$$

$$\frac{u'(\xi,\tau)}{a_0\Delta} = -\xi_0\int_0^\infty \left\{e^{-\sigma_0\kappa\tau} - e^{-\sigma_r\kappa\tau}\left[\cos(\sigma_i\kappa\tau) - \left(\frac{\sigma_0-\sigma_r}{\sigma_i}\right)\sin(\sigma_i\kappa\tau)\right]\right\}$$
$$\times\frac{J_1(\kappa\xi)J_1(\kappa\xi_0)}{(1+2\beta_r)}\left(\frac{\sigma_0}{1+\gamma\sigma_0^2}\right)d\kappa, \tag{32}$$

$$\frac{p'(\xi,\tau)}{\gamma p_0\Delta} = \xi_0\int_0^\infty \left\{e^{-\sigma_0\kappa\tau} - e^{-\sigma_r\kappa\tau}\left[\cos(\sigma_i\kappa\tau) + \left(\frac{\sigma_r^2+\sigma_i^2-\sigma_0\sigma_r}{\sigma_0\sigma_i}\right)\sin(\sigma_i\kappa\tau)\right]\right\}$$
$$\times\frac{J_0(\kappa\xi)J_1(\kappa\xi_0)}{(1+2\beta_r)}\left(\frac{\sigma_0^2}{1+\gamma\sigma_0^2}\right)d\kappa. \tag{33}$$

For constant pressure and $\xi_0 \ll 1$, (31) reduces to the thin gas solution (28). In the constant pressure, optically thick gas limit, the temperature perturbation reduces to

$$\frac{T'}{T_0\Delta} \to \xi_0\int_0^\infty [\exp(-\tfrac{1}{3}\tilde{\tau}\kappa^2)]J_0(\kappa\xi)J_1(\kappa\xi_0)\,d\kappa, \tag{34}$$

which is equivalent to the heat conduction solution given on p. 260 of Carslaw & Jaeger (1959). Constant density forms of (28) and (34) are obtained by replacing $\tilde{\tau}$ by $\gamma\tilde{\tau}$.

Solutions for spherically symmetric problems may be constructed by integrating the sinusoidal functions over the appropriate hemispherical solid angle. These integrals over solid angle reduce to integrals of $\sin\theta\cos(kr\cos\theta)$ and $\cos\theta\sin\theta\sin(kr\cos\theta)$ over θ, where r now denotes the spherical radius. Integration yields elementary solutions proportional to

$$(kr)^{-1}\sin kr \quad \text{and} \quad (kr)^{-2}(\sin kr - kr\cos kr).$$

After applying Fourier sine transform theory to evaluate $b_0(k)$, the following solution is obtained

$$\frac{T'}{T_0\Delta} = \frac{2}{\pi}\int_0^\infty \{e^{-\sigma_0\kappa\tau} + 2e^{-\sigma_r\kappa\tau}[\beta_r\cos(\sigma_i\kappa\tau)+\beta_i\sin(\sigma_i\kappa\tau)]\}$$
$$\times\frac{\sin\kappa\xi\,(\sin\kappa\xi_0 - \kappa\xi_0\cos\kappa\xi_0)}{(1+2\beta_r)\kappa^2\xi}\,d\kappa, \tag{35}$$

$$\frac{u'(\xi,\tau)}{a_0\Delta} = -\frac{2}{\pi}\int_0^\infty \left\{e^{-\sigma_0\kappa\tau} - e^{-\sigma_r\kappa\tau}\left[\cos(\sigma_i\kappa\tau) - \left(\frac{\sigma_0-\sigma_r}{\sigma_i}\right)\sin(\sigma_i\kappa\tau)\right]\right\} \times \frac{(\sin\kappa\xi - \kappa\xi\cos\kappa\xi)(\sin\kappa\xi_0 - \kappa\xi_0\cos\kappa\xi_0)}{(1+2\beta_r)\kappa^3\xi^2}\left(\frac{\sigma_0}{1+\gamma\sigma_0^2}\right)d\kappa, \quad (36)$$

$$\frac{p'(\xi,\tau)}{\gamma p_0\Delta} = \frac{2}{\pi}\int_0^\infty \left\{e^{-\sigma_0\kappa\tau} - e^{-\sigma_r\kappa\tau}\left[\cos(\sigma_i\kappa\tau) + \left(\frac{\sigma_r^2+\sigma_i^2-\sigma_0\sigma_r}{\sigma_0\sigma_i}\right)\sin(\sigma_i\kappa\tau)\right]\right\} \times \frac{\sin\kappa\xi\,(\sin\kappa\xi_0 - \kappa\xi_0\cos\kappa\xi_0)}{(1+2\beta_r)\kappa^2\xi}\left(\frac{\sigma_0^2}{1+\gamma\sigma_0^2}\right)d\kappa, \quad (37)$$

where $\xi \equiv \alpha_0 r$ is now based on the spherical radius.

The temperature perturbation (35) reduces to (28) in the constant pressure, thin gas limit. In the constant pressure, thick gas limit,

$$\frac{T'}{T_0\Delta} \to \frac{1}{2}\left[\operatorname{erf}\left\{\left(\frac{3}{4\tilde{\tau}}\right)^{\frac{1}{2}}(\xi_0+\xi)\right\} + \operatorname{erf}\left\{\left(\frac{3}{4\tilde{\tau}}\right)^{\frac{1}{2}}(\xi_0-\xi)\right\} - \left(\frac{4\tilde{\tau}}{3\pi}\right)^{\frac{1}{2}}\frac{1}{\xi}\left(\exp\left\{-\left(\frac{3}{4\tilde{\tau}}\right)(\xi_0-\xi)^2\right\} - \exp\left\{-\left(\frac{3}{4\tilde{\tau}}\right)(\xi_0+\xi)^2\right\}\right)\right], \quad (38)$$

which is equivalent to the heat conduction solution given on p. 257 of Carslaw & Jaeger (1959).

Evaluation of the integrals for the cylindrical and spherical cases would yield profiles similar to the ones shown in figures 4–9. Three-dimensional effects allow progressively more rapid transport of heat and mass in the cylindrical and spherical cases, therefore, perturbations will decay progressively faster (cf. the conduction solutions shown in Carslaw & Jaeger 1959).

The authors gratefully acknowledge help from Mrs Marielle Bryant with the programming of the numerical integrations. This research was supported by the Advanced Projects Agency of the Department of Defense and was monitored by the U.S. Army Research Office, Durham under Contract DA-31-124-ARO-D-257.

REFERENCES

Baldwin, B. S. 1962 *NASA* TR R-138.

Bathla, P. S. & Viskanta, R. 1968 *Appl. Sci. Res.* **19**, 182.

Calvert, J. B., Coffman, J. W. & Querfeld, C. W. 1966 *J. Acoust. Soc. Am.* **39**, 532.

Carslaw, H. S. & Jaeger, J. C. 1959 *Conduction of Heat in Solids*, 2nd edition, pp. 53–5. Oxford University Press.

Cogley, A. C. 1968 Ph.D. Thesis, Stanford University.

Gille, J. C. 1968 *J. Atmos. Sci*, **25**, 808.

Golitsyn, G. S. 1963 *Bull. Acad. Sci. USSR, Geophys. Ser.* (English Trans.), 589.

Goody, R. M. 1964 *Atmospheric Radiation, Part I*, pp. 344–350. Oxford University Press.

Goody, R. M. & Belton, M. J. S. 1967 *Planet. Space Sci.* **15**, 247.

Lick, W. 1964 *J. Fluid Mech.* **18**, 274.

Moore, F. K. 1966 *Phys. Fluids*, **9**, 70.

Pai, S. I. 1963 *Phys. Fluids* **6**, 1440.

PROKOF'EV, V. A. 1957 *Prikl. Mat. i Mekh.* **21**, 775.

PROKOF'EV. V, A. 1961 *ARS Journal* (English Trans.) **31**, 988.

RIAZANTSEV, I. S. 1959 *J. Appl. Math. Mech.* (USSR, English Trans.) **23**, 1126.

SASAMORI, J. & LONDON, J. 1966 *J. Atmos. Sci.* **23**, 543.

SFORZA, P. M. & PORTER, L. D. 1968 *AIAA J.* **6**, 2267.

SMITH, P. W. 1957 *J. Acoust. Soc. Am.* **29**, 693.

SOLAN, A. & COHEN, I. M. 1966 *Phys. Fluids*, **9**, 2365.

SPIEGEL, E. A. 1957 *Astrophys. J.* **126**, 202.

STEIN, R. F. & SPIEGEL, E. A. 1967 *J. Acoust. Soc. Am.* **42**, 866.

STOKES, G. G. 1851 *Phil. Mag.* **1**, 305.

VETLUTSKII, V. N. & ONUFRIEV, A. T. 1962 *Zh. Prikl. Mekhan. i Tekhn. Fiz.* (*PMFT*), no. 6, 29.

VINCENTI, W. G. & BALDWIN, B. S. 1962 *J. Fluid Mech.* **12**, 449.

VINCENTI, W. G. & KRUGER, C. H. 1965 *Introduction to Physical Gas Dynamics*, pp. 485–505. New York: John Wiley.

ZEL'DOVICH, Y. B. & RAIZER, Y. P. 1967 *Physics of Shock Waves and High-Temperature Hydrodynamic Phenomena*, vol. 2 (English Trans.), pp. 626–51. New York: Academic.